Electronic Supporting Information for

Model-Based Exploration of the Drivers of Mountain Cold-Trapping in Soils

John N. Westgate and Frank Wania*

Department of Chemistry and Department of Physical and Environmental Sciences, University of Toronto Scarborough, 1265 Military Trail, Toronto, Ontario, Canada M1C 1A4

*Corresponding author e-mail: frank.wania@utoronto.ca
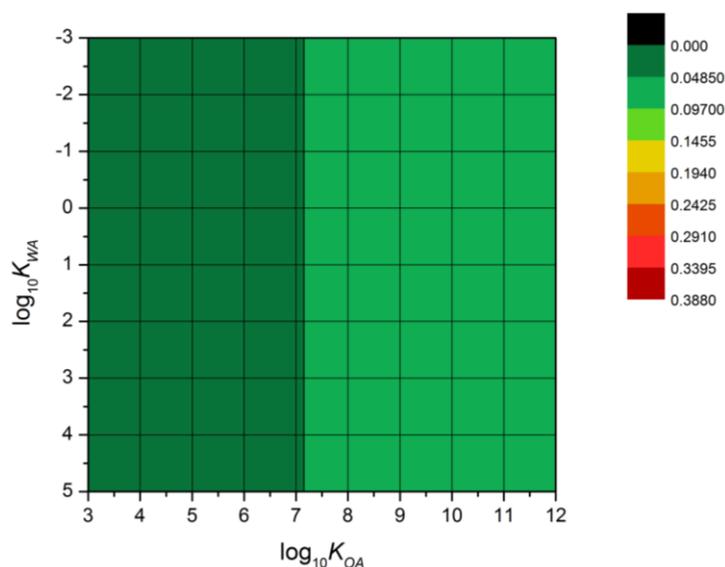
Figure S1 - With no discernible differences between zones and only dry-deposition as a mechanism, MCP_{25} can still reach almost 10%, representing equal soil concentrations in all zones. Note that this is scaled to the same maximum as Figure 4 in the main text. Removing the temperature gradient as well as precipitation and particles should 'shut-down' preferential dry-gaseous deposition, and it should act to the same extent in all zones. What it reveals is the bias for soils intentionally built into the definition of MCP: by including only soils in the numerator and both soils and atmosphere in the denominator, the greater a PPP's affinity for soil, the greater its MCP will be, all else being equal.

A Note on Simulations Run to Near-Steady-State

We assumed that near steady-state was reached when the identity of the PPP with the highest MCP remained the same and its MCP changed by less than 10^{-4} between adjacent one-year blocks of simulated time. Because only the PPP with the highest MCP is considered in the criterion, the MCP of any or all other PPPs could still be changing at any rate. Again, the model is dynamic: the reason that this pseudo-steady-state is attainable is that emissions are steady and unending.

The CSPs for MCP_{SS} for the Scale Scenarios can found in Figure S. The 12 km PEAK reached steady-state after 65 years. The larger mountains require more years of simulation to reach steady-state: the RANGE (Figure Se), REGION (Figure Sf) and HEMISPHERE (Figure Sg) mountains take 85, 220 and 920 years, respectively. The additional 20 years of simulation does not appreciably change the PPPs that exhibit the highest MCP in the RANGE scenario. In the REGION and HEMISPHERE scenarios the additional simulation time gives a slight increase to the $\log_{10} K_{WA}$ and $\log_{10} K_{OA}$ with the highest MCPs. It appears that the K_{WA} band and the K_{OA} band of the CSP for the longer mountains are creeping toward the values from the smaller mountains with increased simulation time. However, because the shift is very slow the arbitrary criterion for near-steady-state is reached and the simulations are terminated.
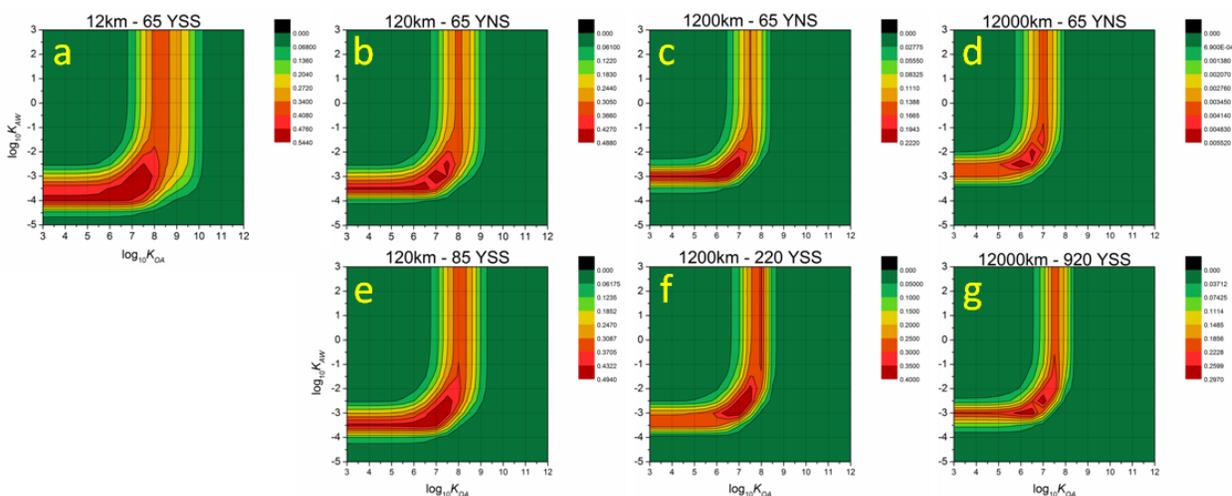
Figure S2 - Chemical space plots for the Scale scenarios, both at a non-steady state after 65 years (denoted 65 YNS) or at near-steady- after further years of simulation (denote with the number of years of simulation followed by YSS). Note that the left axis is $\log_{10} K_{AW}$ (not K_{WA} as in the main text) but as the axis is not reversed the two are directly comparable. Note also that each sub-figure is coloured to its own maximum.

In comparing MCP at either near-steady state, or after very long model runs, the K_{OA} band occurs at higher $\log_{10} K_{OA}$ in the NORAIN, TOPRAIN and BOTRAIN scenarios than the base 120 km scenario and the LESSRAIN and MORERAIN scenarios (Figure S). As with the Scale Scenarios, the main commonality is the length of the model run: longer run times lead to higher K_{OA} being assigned high MCP values. In general, scenarios in which MCP_{MAX} appears most strongly associated with a K_{WA}, the model runs come to steady-state relatively quickly. Scenarios in which a K_{WA} band is weak or absent tend to come to steady-state less quickly, or not at all, in a reasonable run time (<1000 years). It is likely that were near-steady-state defined such that all PPPs were not experiencing changes in MCP (rather than just that with MCP_{MAX}) that no simulation would come to steady state.
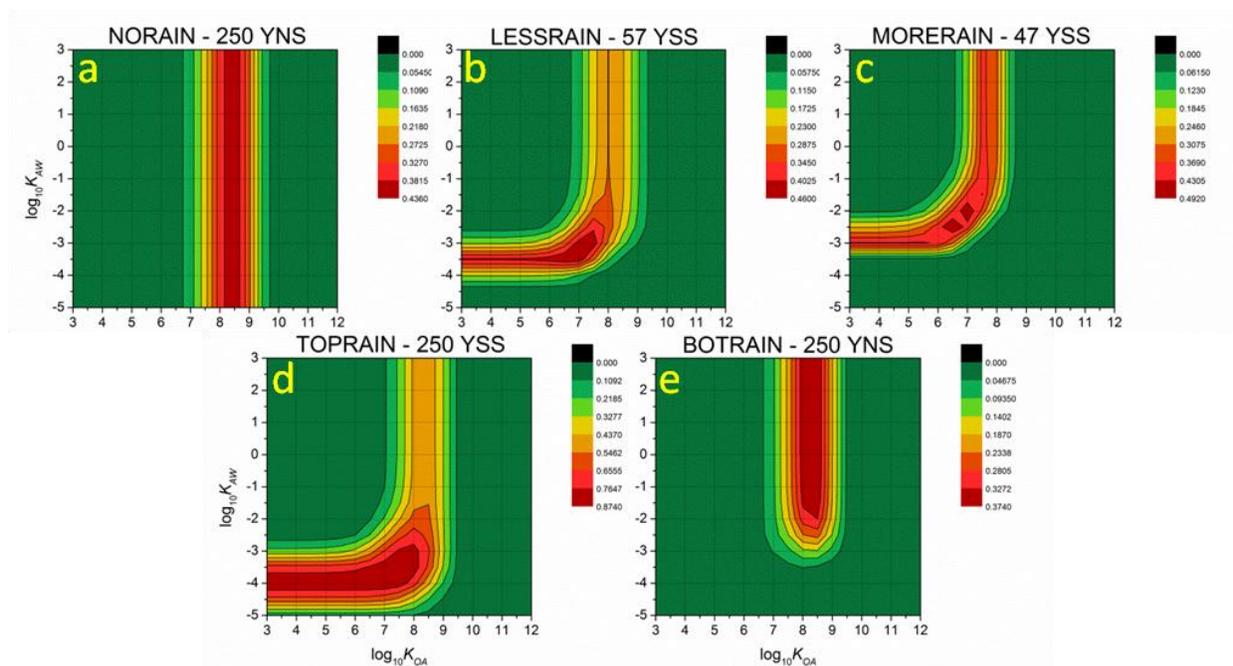
Figure S3 - CSPs of MCP at various lengths of simulation - YSS indicates number of years to steady state. The NORAIN and BOTRAIN scenarios never reached a steady state and were simply terminated. Note that these are not recoloured to a common scale, but that each sub-figure is normalized to its own MCP_{MAX}

The LESSPART scenario came to near-steady-state in 57 years, less than the 85 years under the default condition for the same dimensions (Figure S). The MOREPART scenario required 200 years to reach steady-state again reflecting that wet gaseous processes come to a near-steady-state more quickly than the combination of dry gaseous and particle bound processes.
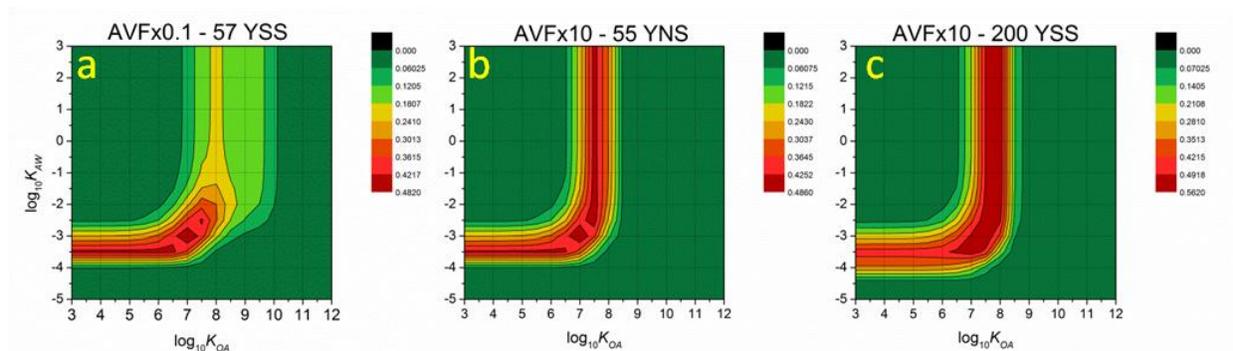
Figure S4 – CSPs of the Particle Scenarios run to steady state (a and c) or terminated at the same time the other reached steady state (b) and coloured normalized to their own maxima. Data were only captured every 5 years in the (b) simulation, thus 55 rather than 57 years. Aerosol Volume Fraction (AVF) refers to particles only and is identical to PVF in the main text.

A Note on the Effect of ΔU_{OA} and ΔU_{AW} on Mountaintop Contamination Potential

Meyer and Wania[1] ran a sensitivity analysis on the GloboPOP model and found that certain areas of the chemical space were very sensitive to changes in ΔU_{OA} and ΔU_{WA}. It was thus expected that by improving the model using calculated energies of phase transfer, as outlined by Gouin et al.,[2] the CSPs of MCP would be notably different from results with fixed values, at least in some areas. Gouin et al. regressed ΔU_{OA} against $\log_{10} K_{OA}$ for a handful of chemicals for which both were available in the literature[3,4] and found a roughly linear relationship. From that they devised the following relationship for calculating ΔU_{OA} (in Joules mol^{-1}) for PPPs:

$$\Delta U_{OA} = -8000 \times \log K_{OA} - 15000 \ldots \text{Equation S1}$$

Setting ΔU_{OW} at a constant -20 kJ·mol^{-1} and assuming internal consistency, ΔU_{AW} can be calculated:

$$\Delta U_{AW} = \Delta U_{OW} - \Delta U_{OA} \ldots \text{Equation S2}$$

Gouin et al. point out that the accuracy of these relationships in the whole chemical space is unknown, in part because they are generated from a regression in only one dimension in the chemical space, and with a very limited number of chemicals. The one-dimensionality means that the calculated ΔU_{AW} values have the odd property of changing with K_{OA} but being independent of K_{AW}.

Figure S allows a comparison of the CSPs with and without this change for four scenarios: the DEFAULT scenario, the TOPRAIN scenario, the MAXdT scenario and the NOdT20 scenario. The second two are included as they are scenarios with the greatest MCPs that span a range of K_{OA} values. A chief difference in the first three scenarios is that with the calculated ΔUs the K_{WA} band does not simply remain the same as K_{OA} changes; MCP decreases as K_{OA} becomes relatively small. Recall, with the calculated values both ΔU_{WA} and ΔU_{OA} vary only with K_{OA} making a physical interpretation challenging. At the lowest K_{OA} both ΔUs are at their smallest meaning PPPs in this area are resistant to phase changes, preventing them from undergoing temperature dependent precipitation scavenging within the range of temperatures modelled. Removing the temperature change with a re-run of the NOdt20 scenario with calculated ΔUs removes the tapered shape and the K_{OA} band extends to the lowest K_{OA} without MCP declining: that is, without a temperature difference the energy of phase transfer becomes superfluous.

Analogous to the wash-out phenomenon, MCP$_{MAX}$ is lower in the NORAIN scenario as well (not shown), perhaps reflecting greater movement to the particle phase and subsequent deposition in the lower zones of the mountain. In fact, all scenarios run with the calculated ΔUs had lower MCP$_{MAX}$ than the corresponding scenarios run with fixed energies of phase transfer.

CSPs for the calculated ΔUs did not differ in the location of the K_{OA} or K_{WA} bands except for the TOPRAIN scenario. In that case, the only one in which MCP$_{MAX}$ still sat clearly along the K_{WA} band, the band shifted towards the water by a half-log unit. This suggests that temperature still plays an important role in the TOPRAIN scenario, despite the extremely favourable rain gradient for upslope enrichment – that is, it is still cold-trapping that drives the MCP, not just precipitation.

It should be pointed out that few real chemicals fall in the area of the CSP most affected by the improvement.[5] Those that do are likely to be ionisable and are thus not modelled properly by the current version of MountainPOP, or are not expected to be sufficiently persistent to exhibit mountain cold-trapping.
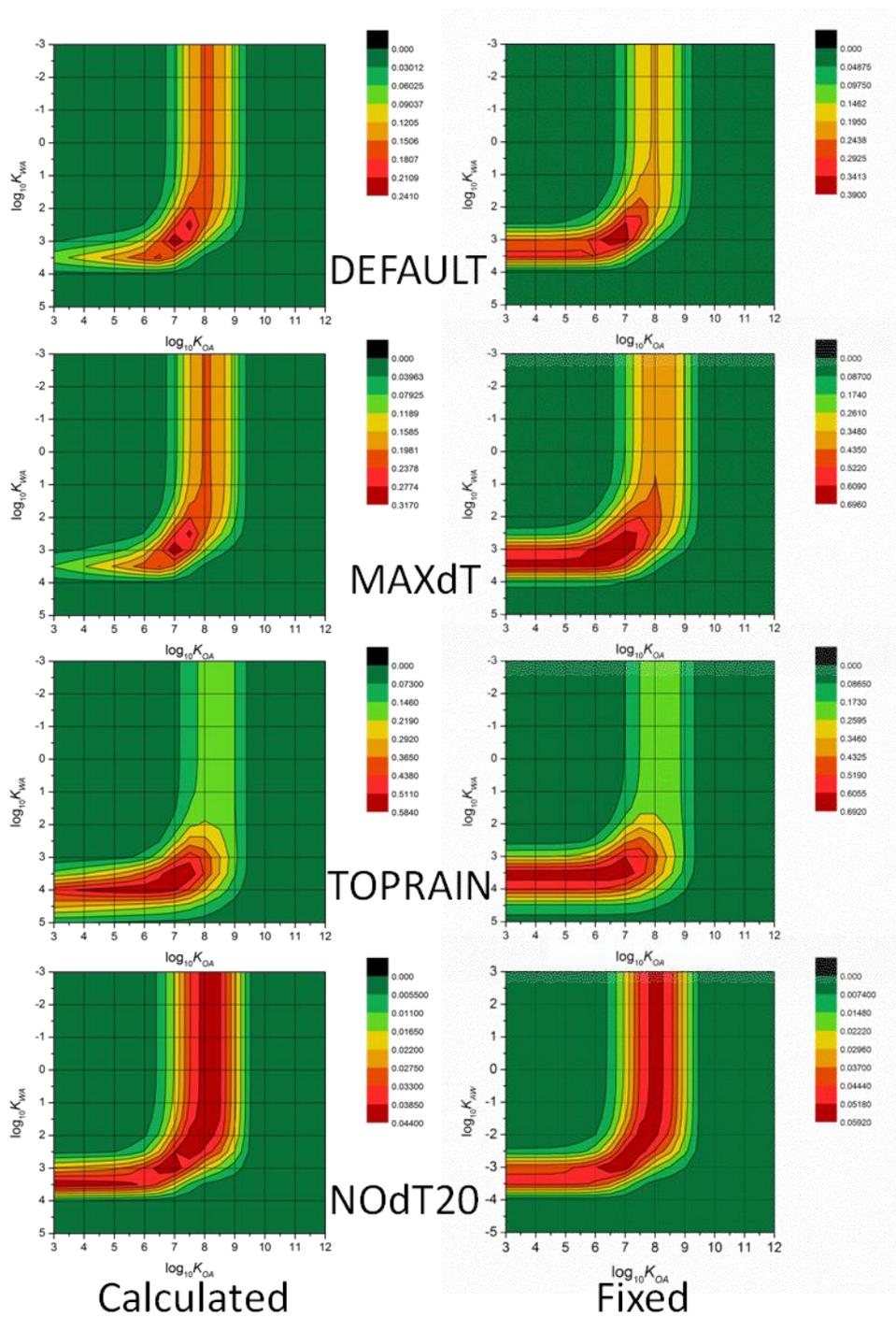
Figure S5 - CSPs for four scenarios using the calculated (left) and fixed (right) energies of phase transfer.

A Note on Soil Moisture

The NORAIN scenario revealed a weakness in the current version of MountainPOP. Soil moisture is quantified in the model simply as the fraction of soil pore space filled with water (v/v). Because for these simulations rain is constant – it rains a little bit all the time rather than periodically raining strongly – a dynamic treatment of soil moisture is unnecessary and soil moisture is simply a constant as well. Such an approach to rain has been criticized as likely to underestimate revolatilization from soils [6], but as this work does not attempt to model actual concentrations on real mountains this concern does not apply here. However, when the NORAIN scenario was run with the default soil conditions species with the very lowest K_{AW}s modeled were assigned values of Mountaintop Contamination Potential (MCP) above the minimum. When the soil moisture was set to an arbitrarily small number and the NORAIN scenario re-run, the result is as pictured in the Figure 4 in the main body of the paper. That is, the most water soluble species were partitioning strongly into the soil water when it was available and rain was not.

A Note on the Relative Contribution of Dry and Wet Particle Deposition to MCP

The magnitudes of MCP in the BOTRAIN and TOPRAIN scenarios provide a clue about the relative importance of dry and wet particle bound deposition. The BOTRAIN scenario has a MCP_{MAX} of 0.37, entirely dictated by dry deposition. The same band of K_{OA} in the TOPRAIN scenario has MCPs between 0.44 and 0.54, ignoring the area where the contributions from all processes overlap. This suggests that for those PPPs whose high MCPs are dependent on their K_{OA}, dry deposition processes are the main drivers. The concentration of PPP that is wet scavenged moves from the numerator to the denominator of the MCP between the TOPRAIN the BOTRAIN scenarios, partially masking the difference. However, it could be that the total mass remaining in the model in the BOTRAIN scenario is considerably less than in TOPRAIN, which would inflate the MCP values.

A look at the time-series of MCP for a sinusoidal emission scenario that peaks at 25 years offers other clues about the processes controlled by K_{OA} (http://www.utsc.utoronto.ca/~westgate/MCPinTime.gif, note that the first image is the end of year 1, the second year 5, after which images are every 5 years to the last year of simulation). At first only PPPs that partition quite strongly to octanol, a surrogate for organic matter both in the soil and in particles, exhibit high MCP. This band moves to lower K_{OA} and then becomes relatively less important than the wet gaseous processes so it is only a wide band of low values. Well after emissions have ceased a second K_{OA} band appears for highly volatile species. More than 99% of the masses of these are found in the soil of the highest zones, because the cool temperatures allow the best retention by the soil at the top, but those masses are vanishingly small.

A Note on the Role of Temperature Gradients in Upslope Enrichment on a Global Scale Mountain

In the main paper we discuss that a gradient in temperature is not required to identify which PPPs are most likely to exhibit upslope enrichment, but that without that gradient insufficient masses of PPPs are trapped and upslope enrichment does not actually occur. This is with the one exception of a mountain on which only dry-gaseous deposition occurs and where PPPs are constantly emitted for scores of years.

Others have suggested that a gradient in temperature is not required to explain differential distributions of contaminants on a global scale, and that, at least in the atmosphere, distance, through differential deposition, is sufficient to drive global fractionation.[7] Furthermore, the same fractionation was seen in their simulations with the temperature gradient reversed (by emitting only in the highest Polar zone). An important difference between that work and this is that concentrations in surface media were not considered in the former, while MCP is defined by concentrations in soil. Nonetheless, simulations with the Global scale mountain (12000 km long) using both the MAXdT scenario and a reversed temperature gradient, REVdT were run to probe for similarities.

As with the 120 km mountain, the identities of the PPPs exhibiting MCP_{MAX} on the 12000 km mountain did not change with the increased range of temperatures between the default and MAXdT, but the value of MCP_{MAX} approximately doubled, for the same length of simulation (Figure S6a). REVdT, on the other hand, made a larger difference: MCP_{MAX} was assigned to the K_{OA} band, rather than the K_{WA} band, and both bands were shifted to more volatile PPPs. To become enriched upslope PPPs must be sufficiently volatile to not be efficiently scavenged from the atmosphere and trapped in the surface media at the lower temperature low on the mountain (Figure S6b). Furthermore, as MCP_{MAX} in this scenario is an order of magnitude smaller than the default temperatures, it is clear that upslope enrichment does not occur under this reversal of temperature gradient.
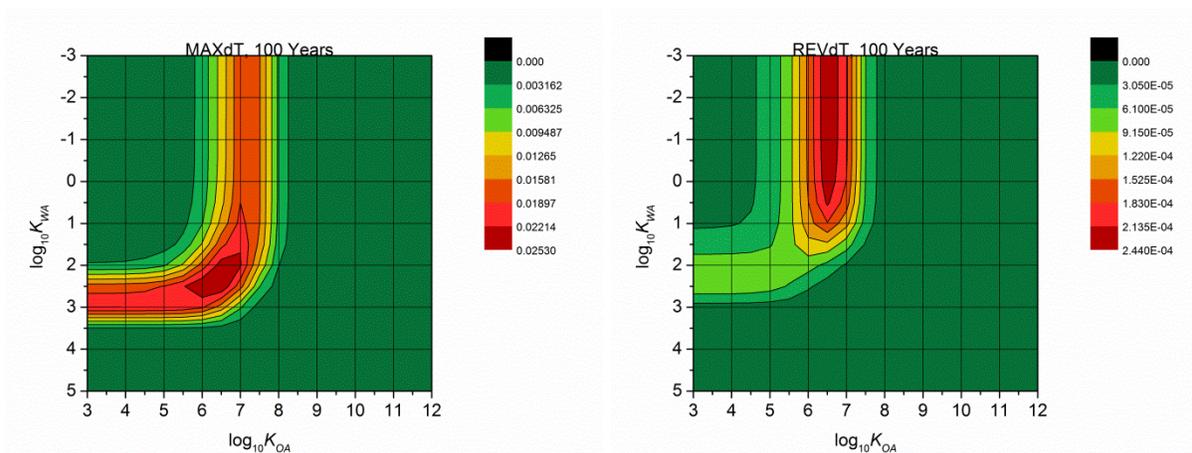
Figure S6 - CSPs for the global scale mountain under the MAXdT and REVdT scenarios: the MCP scales are different as the REVdT produces two orders of magnitude smaller MCP_{MAX} values, meaning it does not produce upslope enrichment.

References

1. T. Meyer and F. Wania, *Atmos. Environ.*, 2007, **41**, 2757–2767.

2. T. Gouin, J. M. Armitage, I. T. Cousins, D. C. G. Muir, C. A. Ng, L. Reid, and S. Tao, *Environ. Toxicol. Chem.*, 2013, **32**, 20 – 31.

3. A. Beyer, F. Wania, T. Gouin, D. Mackay, and M. Matthies, *Environmental Toxicology*, 2002, **21**, 941–953.

4. U. Schenker, M. Macleod, and M. Scheringer, *Environ. Sci. Technol.*, 2005, **39**, 8434–8441.

5. T. N. Brown and F. Wania, *Environ. Sci. Technol.*, 2009, **43**, 6676–6683.

6. E. G. Hertwich, *Environ. Sci. Technol.*, 2001, **35**, 936–940.

7. H. von Waldow, M. MacLeod, K. Jones, M. Scheringer, and K. Hungerbühler, *Environ. Sci. Technol.*, 2010, **44**, 6183–6188.